

FABRICATION OF TiO₂/DYE-SENSITIZED SOLAR CELLS (DSCs) USING DYE EXTRACTS AND THEIR MIXTURE AS PHOTSENSITIZERS

ABSTRACT

In this work we have reported an investigation on *Hibiscus sabdariffa* and *Delonix regia* dye extracts and their mixture as natural sensitizers for TiO₂/DSCs. A shift in the absorption maximum toward the lower energy of the ultraviolet-visible spectrum was observed for the dye mixture and a shift in the absorption maximum towards the higher energy of the ultraviolet-visible spectrum was observed for the dye extracts. The optical band gaps obtained at the point where the absorption spectra showed strong cut offs range from 1.79eV to 2.40eV. Also, we have used TiO₂ thin films of thickness 5.2μm and the Light Harvesting Efficiencies (LHE) of the dye extracts and the dye mixture adsorbed onto TiO₂ surface were close to unity. The average diameter of the TiO₂ films obtained from SEM is in the range of 25-40nm reflecting that the TiO₂ films are transparent and suitable for DSC application. The XRD pattern revealed the TiO₂ films to be of anatase form and the structure type is tetragonal with 3.53217Å as the *d-spacing* for the most prominent peak, $2\theta=25.2139^\circ$ (ICDD data file: 01-075-8897). Three (3) DSCs each of 0.52 cm² active area were assembled and subjected to current-voltage characterization using a standard overhead Veeco viewpoint solar simulator equipped with AM 1.5 filter to give a solar radiation of 1000 W/m² and coupled to Keithley source meter (model 4200SCS). The photoelectrochemical performance of the fabricated DSCs showed open-circuit voltages (V_{oc}) varied from 0.42 to 0.53 V, the short-circuit current densities (J_{sc}) ranged from 0.10mAcm⁻² to 0.90mAcm⁻² and the fill factors (FF) varied from 12 to 38%. The best overall solar power conversion efficiency of 0.13% was obtained, under AM 1.5 irradiation and a maximum short circuit current density of 0.90mAcm⁻². Nevertheless, pure *Hibiscus sabdariffa* and *Delonix regia* dye extracts proved to be rather poor sensitizers as can be seen by the low spectra absorption at lower energies with current densities of 0.17mAcm⁻² and 0.10mAcm⁻² respectively. The solar power conversion efficiencies for *Hibiscus sabdariffa* and *Delonix regia* dye extracts were 0.01% and 0.02% respectively. In our earlier studies, we highlighted an established fact that raw natural dye mixtures exhibit better performance than pure dye extracts. Thus, the power conversion efficiency of 0.13% observed for the dye mixture sensitized TiO₂/DSC corresponds to an increment in the neighborhood of 85% to 92% over the pure dye extracts sensitized TiO₂/DSCs.

Keywords: Natural dyes, dye mixture, light harvesting efficiency, molar extinction coefficient, TiO₂-DSC, optical band gap, power conversion efficiency.

1.0 INTRODUCTION

The power conversion efficiencies of natural dye-sensitized solar cells are low compared to solar cells sensitized with inorganic and synthetic dyes [1, 2, 3]. This is due to weak bonding between the natural dyes and TiO₂ surface which ultimately leads to low short circuit current density deliverable by the solar cells [4]. Other reasons include transformation of the natural dye functional groups from a more stable state (flavilium state) to an unstable state (quinoidal state) upon attachment to the TiO₂ surface which is as a result of high pH values [5, 6, 7]. This unstable state is usually characterized by long bond length functional groups that prevent dye molecules from arraying effectively on the TiO₂ film thereby causing low electron transfer from the dye

43 molecules to the conduction band of TiO_2 . Finally, the masking and agglomeration effects of
44 natural dyes which limit the light harvesting efficiency to ultraviolet and the onset of the visible
45 light spectrum [5, 7, 8, 9, 10].

46
47 Several research efforts have been made to improve the interaction between the natural dyes and
48 TiO_2 surface in order to achieve high power conversion efficiency. These include the use of
49 appropriate extraction solvents, synergistic effect of dyes derived from single species such as
50 algal derived photosynthetic pigments, organic acids and mixed dyes [11, 12, 13, 14, 15, 16, 17,
51 18, 19]. Thus, it was established that mixed dye system would account for many possible types
52 of interactions between dyes with various constituents present, but this is yet to be thoroughly
53 understood [20]. Although, there could be more possible ways to increase the efficiency of solar
54 cells sensitized with natural pigments but it is evident from the equation for power conversion
55 efficiency [equation (1) below] that high values of short circuit current density (J_{sc}), open
56 circuit voltage (V_{oc}) and fill factor (FF) lead to high efficiency in any solar cell. As such, it is
57 necessary to improve these three parameters in order to raise power conversion efficiency of a
58 DSC.

59
60 In our previous studies, we developed and characterized DSC based on TiO_2 nanoparticles
61 coated with Hibiscus sabdariffa (Zobo) and the overall solar power conversion efficiency of
62 0.033% and a maximum current density of 0.17mAcm^{-2} were obtained [21]. Typically, low peak
63 absorption coefficient, small spectra width and very low power conversion efficiency of this
64 DSC boosted additional studies oriented; on one hand, to the use of a new natural sensitizer
65 (*Delonix regia*) in addition to Hibiscus sabdariffa and their mixture as a promising strategy for
66 harvesting more light in the higher wavelengths. On the other hand, we hope to increase the
67 extent of Light Harvesting Efficiency (LHE) within the TiO_2 electrode by depositing a blocking
68 layer sequentially to enhance the surface area of TiO_2 , to favor cluster formation in TiO_2 nanoparticles
69 for effective anchorage of the natural dye extracts and their mixture and to improve interconnectivity
70 among TiO_2 nanoparticles for enhancement in the short circuit current density. Sequel to this, three (3)
71 DSCs each of 0.52 cm^2 active area were assembled by sandwiching a surlyn polymer foil of 25
72 μm thickness, as spacer between the photoelectrode and the platinum counter electrode and
73 characterized using a standard overhead Veeco viewpoint solar simulator equipped with AM 1.5
74 filter to give a solar radiation of 1000 W/m^2 and coupled to a Keithley source meter (model
75 4200SCS) which was connected to the computer via GPIB interface for data acquisition.

76
77
78
79

80 2. MATERIALS AND METHODS

81 Titanium isopropoxide, Titanium nanoxide, acetylacetonate, ethanol, isopropanol, fluorine doped
82 tin-oxide (FTO) conducting glass [11.40 ohm/m^2 , $(1.00 \times 1.00)\text{cm}^2$], electrolyte (iodolyte-AN-
83 50), sealing gasket (surlyn-SX1170-25PF), and screen-printable platinum catalyst, (Pt-catalyst
84 T/SP) all were obtained from SOLARONIX. Dye extracts were obtained from the natural
85 products (*Hibiscus sabdariffa* and *Delonix regia*). A mixture of 0.3M of titanium isopropoxide,
86 1.2M acetylacetonate and isopropanol was spin coated three (3) times with different
87 concentrations sequentially as blocking layer on the pre-cleaned fluorine doped tin-oxide (FTO)

88 conducting glasses and sintered at 150°C for four minutes each time the deposition was made.
89 Subsequently, a paste of titanium nanoxide in propanol in the ratio 1:3 was screen printed on the
90 three (3) fluorine doped tin-oxide (FTO) conducting glasses and allowed to dry at 125°C in open
91 air for 6 minutes.

92 The FTO/TiO₂ glass electrodes were sintered in a furnace at 450°C for 40 minutes and allowed
93 to cool to room temperature to melt together the TiO₂ nanoparticles and to ensure good
94 mechanical cohesion on the glass surface. Dried leaves of *Hibiscus sabdariffa* and *Delonix regia*
95 were crushed into tiny bits and boiled in 75ml of deionized water for 15 minutes. The residue
96 was removed by filtration and the resulting extracts were centrifuged to further remove any solid
97 residue while a mixture in the ratio 50:50 by volume of the dye extracts was made. The dye
98 extracts and the mixture were used directly as prepared for the construction of the DSCs at room
99 temperature. A scattering layer of TiO₂ was also deposited on the TiO₂ electrodes before the
100 electrodes were immersed (face-up) in the natural dye extracts and their mixture for 18h at room
101 temperature for complete sensitizer uptake. This turned the TiO₂ film from pale white to
102 sensitizer colour. The excess dye was washed away with anhydrous ethanol and dried in
103 moisture free air.

104 The thickness of TiO₂ electrodes and the deposited scattering layers was determined using
105 Dekker Profilometer. Surface morphology of the screen-printed TiO₂ nanoparticles was observed
106 using EVOI MA10 (ZEISS) multipurpose scanning electron microscope operating at 20kV
107 employing secondary electron signals while the corresponding Energy Dispersive Spectra (EDS)
108 were obtained using characteristic x-rays emitted by TiO₂ nanoparticles. The X-ray diffraction
109 (XRD) pattern of the screen-printed TiO₂ nanoparticles at room temperature was recorded using
110 X-ray Diffractometer; Panalytical Xpert-Pro, PW3050/60, operating at 30mA and 40kV, with
111 monochromatic Cu-K α radiation, of wavelength $\lambda = 1.54060\text{\AA}$. A scanned range $3-80.00553^\circ 2\theta$,
112 with a step width of 0.001° was used. The pattern was analyzed and the peaks were identified
113 using ICDD data file (01-075-8897). The UV-Visible (UV-Vis) absorption measurements of the
114 dye extracts, their mixture and the dye extracts and their mixture on the screen printed TiO₂
115 electrodes were carried out with Avante UV-VIS spectrophotometer (model-LD80K). From these
116 measurements, plots for the absorbance, Light Harvesting Efficiency (LHE) and molar extinction
117 coefficient versus the wavelengths of interest were obtained using the relevant expressions from
118 [4].

119 Three (3) DSCs each of 0.52cm^2 active area were assembled by sandwiching a surlyn polymer
120 foil of $25\mu\text{m}$ thickness, as spacer between the photoelectrode and the platinum counter electrode
121 and then hot-pressed at 80°C for 15s. A drop of liquid electrolyte was introduced into the cell
122 assemblies via pre-drilled holes on the counter-electrodes and sealed using amosil sealant. In
123 order to have good electrical contacts, a strip of wire was attached to both sides of the FTO
124 electrodes. Finally, the DSCs were subjected to current-voltage characterization using a standard
125 overhead Veeco viewpoint solar simulator equipped with Air Mass 1.5 (AM 1.5) filter to give a
126 solar radiation of 1000 W/m^2 and coupled to Keithley source meter (model 4200SCS) which was
127 connected to the computer via GPIB interface for data acquisition. Subsequently, the working
128 electrode and counter electrode of the DSC were connected in turn to the positive and negative
129 terminals of the digital Keithley source meter respectively. The bias was from short circuit to
130 open circuit and was obtained automatically using LabVIEW software from National
131 Instruments Inc, USA. From the data, $I-V$ curves were plotted in real time for the DSCs under

132 illuminated condition. Following this, the photovoltaic parameters viz; the open circuit voltage
133 (V_{oc}) and short circuit current (I_{sc}) were obtained from the I - V curves for the cells. The fill factor
134 (FF) and the power conversion efficiency for the cells were obtained using the following
135 relations:

$$136 \quad FF = \frac{P_m}{V_{oc} \cdot I_{sc}} \quad \text{and} \quad \eta = \frac{FF \cdot V_{oc} \cdot J_{sc}}{I_{in}} \quad (1)$$

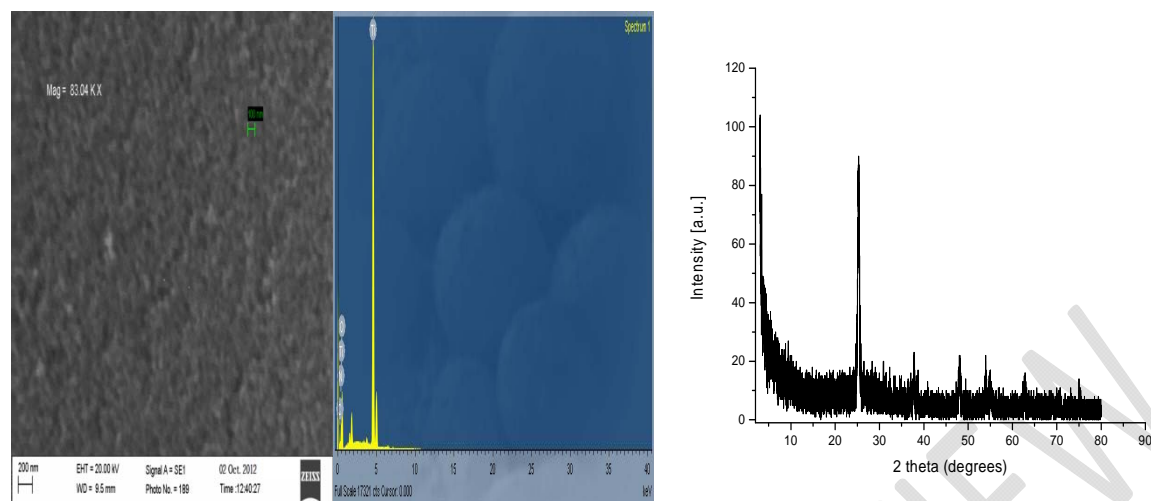
137
138
139
140

3.0 RESULTS AND DISCUSSION

141 The image presented in Figure 1 obtained using characteristic x-rays emitted by TiO_2
142 nanoparticles was observed at a magnification of 83.04kX. The uniform contrast in the image
143 revealed TiO_2 to be practically isomorphous with titanium and oxygen being the dominant
144 elements with concentration of about 99.9% as depicted in the EDS spectra (Figure 1b). The
145 morphology of TiO_2 nanoparticles is such that the particles are closely packed and spherical in
146 shape. The average diameter of the particles is in the range of 25-40nm reflecting that TiO_2
147 nanoparticles are transparent and suitable for DSC application. The thickness of TiO_2 on the
148 FTO conducting glass determined using Dekker Profilometer was found to be 5.2 μm for each
149 photoelectrode and that of the deposited scattering layers was found to be 1 μm . The XRD
150 pattern revealed the compound name for the TiO_2 electrode to be anatase syn., and the structure
151 type is tetragonal with 3.53217 \AA as the d -spacing for the most prominent peak, $2\theta=25.2139^\circ$
152 (ICDD data file: 01-075-8897). Other prominent peaks occur at $2\theta= 37.7883^\circ, 48.0463^\circ,$
153 $53.9110^\circ, 55.0481^\circ, 62.7104^\circ$ and 75.1376° with d -spacing $d= 2.38075 \text{ \AA}, 1.89370 \text{ \AA}, 1.70073 \text{ \AA},$
154 $1.66826 \text{ \AA}, 1.48160 \text{ \AA}$ and 1.26338 \AA .

155
156 In figure 2, the dye extracts and their mixture exhibit absorption maxima slightly above 400nm
157 and the most prominent shoulders occur slightly above 500nm. But upon sensitization on TiO_2 ,
158 there was reduction in absorption maxima and the prominent shoulders for the dye extracts while
159 an enhancement in the absorption maximum with a shift toward high wavelengths (450nm –
160 600nm) was observed for the dye mixture and the prominent shoulder broadened toward the
161 higher wavelengths (750nm – 900nm) with reduced absorption intensity for the mixture.

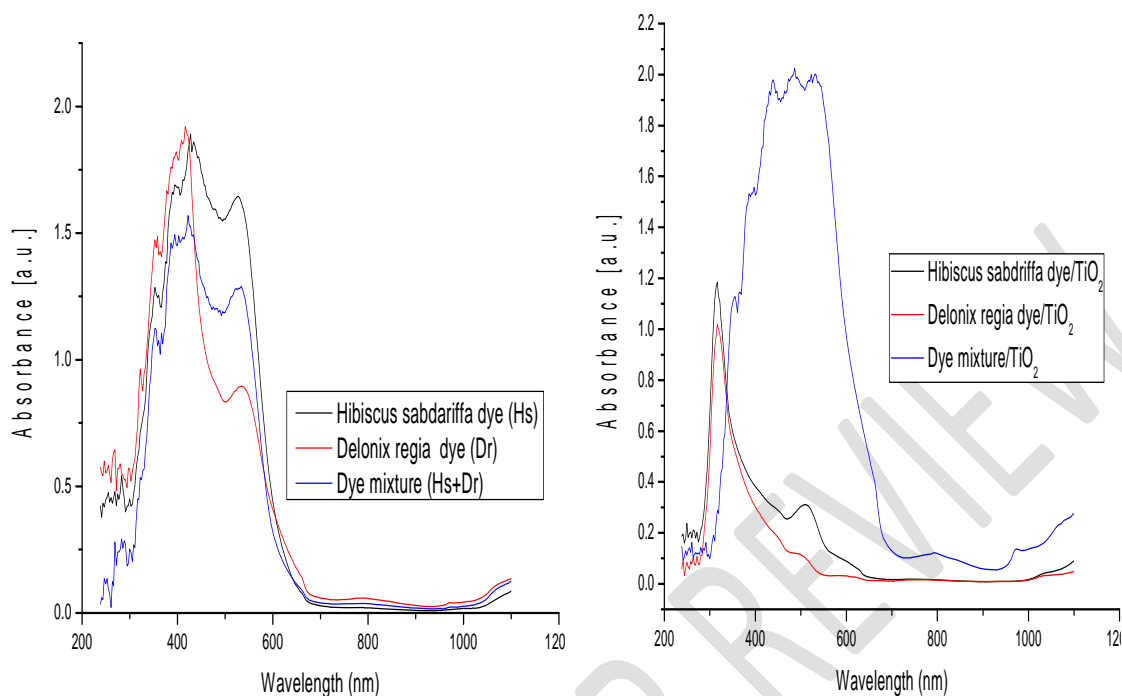
162



163
 164
 165 (a) (b) (c)
 166 Figure 1: TiO_2 structural characteristics: (a) Surface morphology, (b) Energy Dispersive Spectra
 167 and (c) XRD pattern for the screen printed TiO_2 .
 168

169 Chemisorption of anthocyanins on TiO_2 was been reported by [22] to be as a result of alcoholic
 170 bound protons which condense with the hydroxyl groups present at the surface of nanostructured
 171 TiO_2 . Such attachment to the TiO_2 surface stabilizes the excited state, thus shifting the absorption
 172 maximum towards the lower energy of the spectrum. In our study, a shift in the absorption
 173 maximum towards the lower energy of the spectrum was observed for the dye mixture adsorbed
 174 on TiO_2 and a shift in the absorption maximum towards the higher energy of the spectrum was
 175 observed for the dye extracts adsorbed on TiO_2 . This observation suggests that there was
 176 effective adsorption of the dye mixture onto TiO_2 surface which could be attributed to the low
 177 pH value and the short bond length of the OH groups present in the dye mixture. These OH
 178 groups favour the formation a strong bond with the oxide surface and also good arraying to the
 179 TiO_2 film effectively. The shift may also be attributed to the changing of the anthocyanin
 180 molecule from the unstable quinoidal state to the more stable flavilium state to upon chelation.

181 It is an established fact that the light absorption by a dye monolayer is small since the cross
 182 section for photon absorption of most photosensitizers is much smaller than the geometric area
 183 occupied on the semiconductor surface, but with thin film semiconductor the obtainable LHE is
 184 usually close to unity [23]. In this work, we have used TiO_2 thin film of thickness $5.2\mu m$ and the
 185 LHE of the dye extracts and the dye mixture adsorbed onto TiO_2 surface is close to unity.

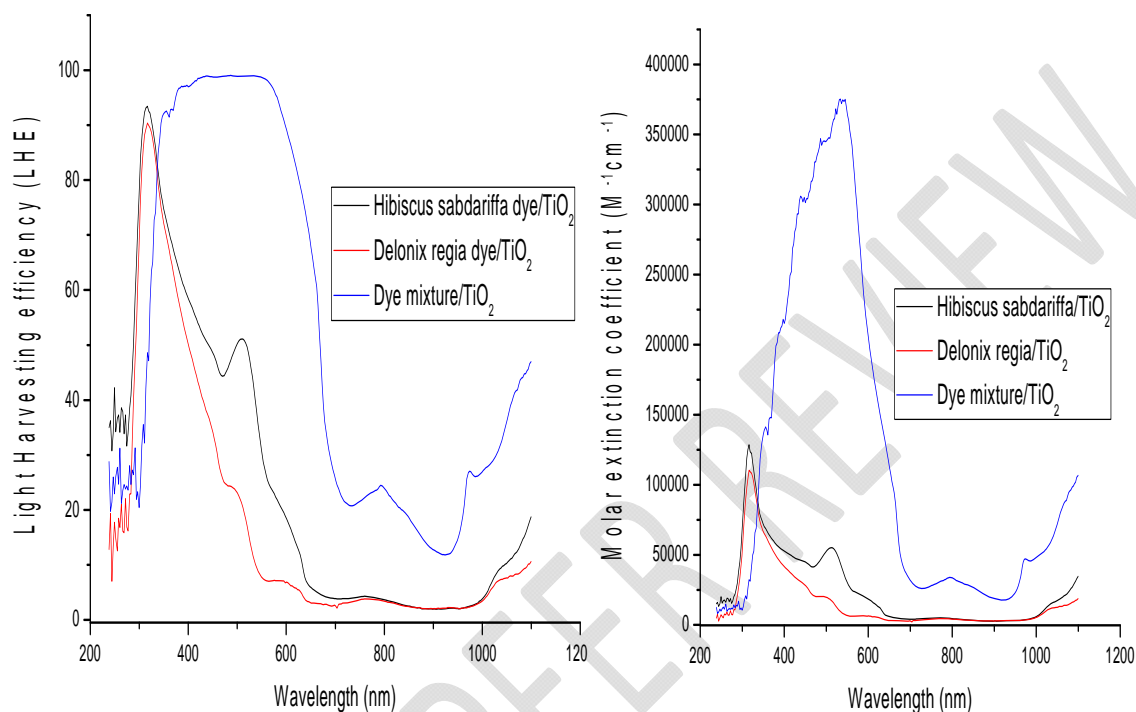


186
 187
 188 Figure 2: UV–VIS absorption spectra for (a) Hibiscus sabdariffa dye extract, Delonix regia dye
 189 extract and Mixture of dye extracts and (b) Hibiscus sabdariffa / TiO₂, Delonix regia/TiO₂ and
 190 Mixture of dye extracts/TiO₂.
 191

192 The light harvesting efficiency values obtained are plotted against wavelengths as shown in
 193 figure 3. The absorption band of the dye extracts after sensitization on TiO₂ becomes a bit
 194 discrete after sensitization but quite broad for the dye mixture after sensitization. Whilst the
 195 molar extinction coefficients are very high for the dye extracts and the mixture, it turned out that
 196 only small areas are being covered by the solar irradiance spectrum for the dye extracts but an
 197 increase in the area was observed for the dye mixture. Most notably, the spectra bandwidth is
 198 within the range of 150nm to 200nm for the dye extracts but an increase in the vicinity of 400nm
 199 to 500nm was observed for the dye mixture. This increase in the spectra bandwidth significantly
 200 enhances the photocurrent density for the dye mixture/TiO₂-DSC as evident from current-voltage
 201 characterization.

202 Current density and power versus voltage characteristics of the DSCs are plotted and shown in
 203 figure 4. The photovoltaic parameters are determined and tabulated in Table 1. The current
 204 density ranges from 0.17mAcm⁻² to 0.90mAcm⁻², the open circuit voltage ranges from 0.42V to
 205 0.53V, the fill factor from 12% to 38% and the power conversion efficiency ranges from 0.01%
 206 to 0.13%. Thus, it is evident from table 1 that high values of J_{sc} , and V_{oc} are responsible for the
 207 higher efficiency obtained for the dye mixture/TiO₂-DSC compared to those of the parent dyes.
 208 In our previous studies, we developed and characterized DSC based on TiO₂ nanoparticles
 209 coated with Hibiscus sabdariffa (Zobo) and the overall solar power conversion efficiency of

210 0.033% and a maximum current density of 0.17mAcm^{-2} were obtained [21]. This boosted
 211 additional studies oriented to the use of dye mixture (Hibiscus sabdariffa plus delonix regia)
 212 leading to an enhancement in the light harvesting efficiency and hence the photocurrent density
 213 which is owed to the high peak absorption coefficient and large spectra bandwidth.

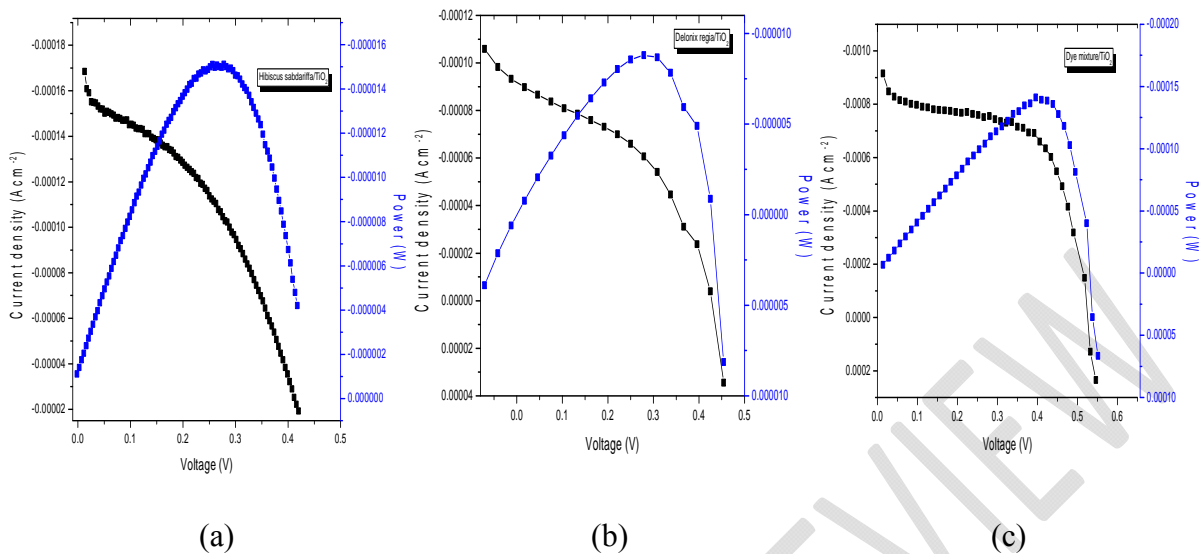


214 Figure 3: Light Harvesting Efficiency (LHE) for (a) Hibiscus sabdariffa / TiO₂, Delonix
 215 regia/TiO₂ and Mixture of dye extracts/TiO₂ and (b) Hibiscus sabdariffa / TiO₂, Delonix
 216 regia/TiO₂ and Mixture of dye extracts/TiO₂.
 217
 218
 219
 220
 221

222 **Table 1: Photovoltaic parameters of the DSCs sensitized with *Hibiscus sabdariffa* dye,**
 223 ***Delonix regia* dye and their mixture**

DSC	$J_{sc}(\text{mAcm}^{-2})$	$V_{oc} (V)$	FF	η (%)
<i>H. sabdariffa</i> /TiO ₂	0.17	0.42	0.12	0.01
<i>Delonix regia</i> /TiO ₂	0.10	0.45	0.38	0.02
<i>Dye mixture</i> /TiO ₂	0.90	0.53	0.28	0.13

224



225

226

227 Figure 4: Current density and Power versus voltage for (a) TiO_2 -DSC sensitized with *Hibiscus*
 228 *sabdariffa* dye, (b) TiO_2 -DSC sensitized with *Delonix regia* dye and (c) TiO_2 -DSC sensitized
 229 with dye mixture.

230

231 In this work, it was discovered that TiO_2 band gap was reduced upon sensitization with the
 232 extracted dyes and their mixture. The optical band gaps were obtained at the point where the
 233 absorption spectra showed a strong cut off, when the absorbance values are minimum. The
 234 values range from $1.79eV$ to $2.40eV$. The band shifts could be attributed to molecular transitions
 235 that take place when the dye molecules chelate with TiO_2 . Typically, anthocyanin dyes exhibit π
 236 $-\pi^*$ orbital transition which is attributed to the wavelength range between $500nm$ to slightly
 237 above $650nm$. In this work, the cut off wavelength for the spectra ranges between $600nm$ to
 238 slightly above $700nm$. Finally, it is well known that proton adsorption causes a positive shift of
 239 the Fermi level of the TiO_2 , thus limiting the maximum photovoltage that could be delivered by
 240 the cells [22]. Nevertheless, the dye mixture proved to be a better sensitizer compared to pure
 241 *Hibiscus sabdariffa* and *Delonix regia* that exhibited low spectral absorption at lower energies.
 242 However, no deviation from this trend was observed when the duration of continuous stimulated
 243 sunlight illumination was increased for several hours.

244

245 4.0 CONCLUSION

246 In this work we have reported an investigation on *Hibiscus sabdariffa* and *Delonix regia* dye
 247 extracts and their mixture as natural sensitizers of $TiO_2/DSCs$. The best overall solar power
 248 conversion efficiency of 0.13% was obtained, under $AM 1.5$ irradiation and a maximum current
 249 density of $0.90mAcm^{-2}$. Nevertheless, pure *Hibiscus sabdariffa* and *Delonix regia* dye extracts
 250 proved to be rather poor sensitizers as can be seen by the low spectral absorption at lower
 251 energies with current density of $0.17mAcm^{-2}$ and $0.10mAcm^{-2}$ respectively. The solar power
 252 conversion efficiency for *Hibiscus sabdariffa* and *Delonix regia* dye extracts are 0.01% and
 253 0.02% respectively. In our earlier studies, we highlighted an established fact that raw natural dye

254 mixtures exhibit better performance than pure dye extracts. Thus, the power conversion
255 efficiency of 0.13% observed for the dye mixture corresponds to 92% and 85% increment over
256 the pure dye extracts sensitized $TiO_2/DSCs$. This could be related to the specific pools of
257 ancillary molecules present in the dye mixture of (*i.e.*, alcohols, organic acids, *etc.*) which act as
258 coadsorbates, suppressing recombination with the electrolyte, reducing dye aggregation and
259 favouring charge injection. Although the efficiencies obtained with this natural dye extracts and
260 the dye mixture are still below the current requirement for large scale practical application, the
261 results are encouraging and may boost additional studies focused on the modification of solar
262 cell components compatible with the dye mixture. In view of this, we are currently exploring the
263 possibility of increasing the power-conversion efficiency of the $DSCs$ based on TiO_2 using
264 modified TiO_2 and counter electrodes and *Delonix regia*.

265
266
267
268
269

270 REFERENCES

271
272

- 273 1. Calogero G, Di-Marco G, Cazzanti S, Caramori S, Argazzi R, Bignozzi CA. Natural dye
274 sensitizers for photoelectrochemical cells. *Energ. Environ. Sci.* 2009. 2, Pp.1162– 1172.
- 275 2. Gong J, Liang J, Sumathy K. Review on dye-sensitized solar cells (DSSCs):
276 fundamental concepts and novel materials. *Renew Sustain Energy Rev.*, 2012. 16(8),
277 Pp.5848–60.
- 278 3. Nazeeruddin MK, Baranoff E, Grätzel M. Dye-sensitized solar cells: a brief
279 overview. *Sol Energy*, 2011. 85(6); Pp.1172–8.
- 280 4. Ooyama Y, Harima Y. Photophysical and electrochemical properties, and molecular
281 structures of organic dyes for dye-sensitized solar cells. *Chem. Phys. Chem.* 2012.
282 13(18); Pp.4032–80.
- 283 5. Narayan MR, Review: dye sensitized solar cells based on natural photosensitizers.
284 *Renew Sustain Energy Rev.*, 2012. 16(1); Pp.208–15.
- 285 6. Teoli F, Luciola S, Nota P, Frattarelli A, Matteocci F, Di Carlo A, Caboni E, Forni C.
286 Role of pH and pigment concentration for natural dye-sensitized solar cells treated
287 with anthocyanin extracts of common fruits. *J Photochem Photobiol A: Chem.*, 2016.
288 316: Pp. 24–30.
- 289 7. Zhou H, Wu L, Gao Y, Ma T. Dye-sensitized solar cells using 20 natural dyes as
290 sensitizers. *J. Photochem Photobiol A: Chem.* 2011. 219(2–3); Pp.188–94.
- 291 8. Wongcharee K, Meeyoo V, Chavadej S. Dye-sensitized solar cell using natural dyes
292 extracted from rosella and blue pea flowers. *Sol. Energy Mater., Sol., Cells.* 2007. 91(7);
293 Pp.566–71.
- 294 9. Palomares E, Clifford JN, Haque SA, Lutz T, Durrant JR. Control of charge
295 recombination dynamics in dye sensitized solar cells by the use of conformally
296 deposited metal oxide blocking layers. *J. Am. Chem. Soc.* 2003.125, Pp. 475–482.
- 297 10. Calogero G, Di-Marco G, Cazzanti S, Caramori S, Argazzi R, Carlo AD, Bignozzi CA.
298 Efficient dye-sensitized solar cells using red turnip and purple wild Sicilian prickly
299 pear fruits. *Int J Mol Sci.*, 2010 1(1); Pp.254–67.

- 300 11. Warkoyo W, Saati EA. The solvent effectiveness on extraction process of seaweed
301 pigment. *Makara Teknol.* 2011. 15(1); Pp.5–8.
- 302 12. Sreekala CO, Jinchu I, Sreelatha KS, Janu Y, Prasad N, Kumar M, Sadh AK, Roy MS.
303 Influence of solvents and surface treatment on photovoltaic response of DSSC based on
304 natural Curcumin dye. *IEEE J Photovolt.* 2012. 2(3); Pp.312–9.
- 305 13. Shahid M, Shahidul I, Mohammad F. Recent advancements in natural dye applications: a
306 review. *J Clean Prod.* 2013. 53; Pp. 310–331.
- 307 14. Prima EC, Yuliarto B, Suendo V. Improving photochemical properties of *Ipomea*
308 *pescaprae*, *Imperata cylindrica* (L.) Beauv, and *Paspalum conjugatum* Berg as
309 photosensitizers for dye sensitized solar cells. *J Mater Sci: Mater Electron.*, 2014.
310 25(10); Pp.4603–11.
- 311 15. Damit DNFP, Galappaththi K, Lim A, Petra MI, Ekanayake P. Formulation of water to
312 ethanol ratio as extraction solvents of *Ixora coccinea* and *Bougainvillea glabra* and
313 their effect on dye aggregation in relation to DSSC performance. *Ionics.* 2017. 23(2);
314 Pp.485–95.
- 315 16. Lindley CC, Bjorkman O. Fluorescence quenching in four unicellular algae with
316 different light harvesting and xanthophyll-cycle pigments. *Photosynth Res.*, 1998. 56(3);
317 Pp.277–289.
- 318 17. Kumara NTRN, Petrovic M, Peiris DSU, Marie YA, Vijila C, Iskander M,
319 Chandrakanthi RLN, Lim, CM, Hobley J, Ekanayake P. Efficiency enhancement of
320 *Ixora* floral dye sensitized solar cell by diminishing the pigments interactions. *Sol*
321 *Energy.* 2015. 117; Pp.36–45.
- 322 18. Hosseinnzhad M. Improvement performance of dye sensitized solar cells from co-
323 sensitisation of TiO₂ electrode with organic dyes based on indigo and thioindigo. *Mater*
324 *Technol.*, 2016. 31(6); Pp.348–51.
- 325 19. Lim A, Damit DNFP., Ekanayake P. Tailoring of extraction solvent of *Ixora coccinea*
326 flower to enhance charge transport properties in dye-sensitized solar cells. *Ionics.* 2015.
327 21(10); Pp.2897–904.
- 328 20. Kumara NTRN, Ekanayake P, Lim A, Liew LYC, Iskander M, Ming LC. Layered co-
329 sensitization for enhancement of conversion efficiency of natural dye sensitized solar
330 cells. *J Alloy Compd.*, 2013. 581(0); Pp.186–91.
- 331 21. Ahmed TO, Akusu PO, ALU N, Abdullahi MB. Dye-Sensitized Solar Cells based on
332 TiO₂ Nanoparticles and *Hibiscus sabdariffa*. *British Journal of Applied Science and*
333 *Technology (BJAST).* 2013. 3(4); Pp.840-846.
- 334 22. Hao S, Wu J, Huang Y. Lin J. Natural dyes as photosensitizers for dye-sensitized
335 solar cell. *Solar Energy.* 2006. 80, 209.
- 336 23. Gratzel M. Solar energy conversion by dye-sensitized photovoltaic cells. *Inorganic*
337 *Chemistry.* 2005. 44, 6841.

338